Development 125, 4007-4017 (1998)
Printed in Great Britain © The Company of Biologists Limited 1998
DEV4974

Atm deficiency results in severe meiotic disruption as early as leptonema of prophase I

Carrolee Barlow[1,*,‡], Marek Liyanage[2,*,§], Peter B. Moens[3], Madalina Tarsounas[3], Kunio Nagashima[4], Kevin Brown[5], Scott Rottinghaus[6], Stephen P. Jackson[6], Danilo Tagle[5], Thomas Ried[2] and Anthony Wynshaw-Boris[1,¶]

[1]Genetic Disease Research Branch, [2]Genome Technology Branch and [5]Molecular Genetics and Biology Branch, National Human Genome Research Institute, National Institutes of Health, Bethesda, MD 20892, USA
[4]Laboratory of Cell and Molecular Structure, SAIC Frederick, NCI-Frederick Cancer Research and Development Center, Frederick, MD 21702, USA
[3]Department of Biology, York University, Downsview, Ontario, M3J 1P3, Canada
[6]Wellcome/CRC Institute, Tennis Court Road, Cambridge CB2 1QR, UK
*The first two authors contributed equally
‡Present address: The Salk Institute for Biological Studies, 10010 North Torrey Pines Road, La Jolla, CA 92037, USA
§Present address: Aurora Biosciences Corporation, 11010 Torreyana Road, San Diego, CA 92121, USA
¶Author for correspondence (e-mail: tonywb@nhgri.nih.gov)

Accepted 29 July; published on WWW 14 September 1998

SUMMARY

Infertility is a common feature of the human disorder ataxia-telangiectasia and *Atm*-deficient mice are completely infertile. To gain further insight into the role of ATM in meiosis, we examined meiotic cells in *Atm*-deficient mice during development. Spermatocyte degeneration begins between postnatal days 8 and 16.5, soon after entry into prophase I of meiosis, while oocytes degenerate late in embryogenesis prior to dictyate arrest. Using electron microscopy and immunolocalization of meiotic proteins in mutant adult spermatocytes, we found that male and female gametogenesis is severely disrupted in *Atm*-deficient mice as early as leptonema of prophase I, resulting in apoptotic degeneration. A small number of mutant cells progress into later stages of meiosis, but no cells proceed beyond prophase I. ATR, a protein related to ATM, DMC1, a RAD51 family member, and RAD51 are mislocalized to chromatin and have reduced localization to developing synaptonemal complexes in spermatocytes from *Atm*-deficient mice, suggesting dysregulation of the orderly progression of meiotic events. ATM protein is normally present at high levels primarily in ova cytoplasm of developing ovarian follicles, and in the nucleus of spermatogonia and to a lesser extent in spermatoctyes, but without localization to the synaptonemal complex. We propose a model in which ATM acts to monitor meiosis by participation in the regulation or surveillance of meiotic progression, similar to its role as a monitor of mitotic cell cycle progression.

Key words: ATM, Meiosis, Prophase I, ATR, DMC1, Electron microscopy, Immunolocalization, Mouse

INTRODUCTION

Reduction from the diploid to haploid state is accomplished by pairing, synapsis, recombination and segregation of homologous chromosomes during meiotic prophase and meiosis I division (reviewed in Kleckner, 1996; Koehler et al., 1996; Roeder, 1997). Interference with one or more of these functions can lead to lethality of reproductive cells or in formation of defective meiotic products, a point that has been well demonstrated in several *Saccharomyces cerevisiae* and *Drosophila melanogaster* mutants (reviewed in Orr-Weaver, 1995; Roeder, 1995).

In addition, targeted inactivation of several mammalian genes has resulted in infertility phenotypes, implicating these genes in processes important in meiosis. For example, we (Barlow et al., 1996) and others (Elson et al., 1996; Xu et al., 1996) described the phenotype of mice with a targeted disruption of *Atm*, the mouse homologue of the human gene (*ATM*) that is mutated in ataxia-telangiectasia (AT). *Atm*-deficient mice recapitulate the phenotype of AT (Boder, 1975; Sedgewick and Boder, 1991), providing an excellent model for this disease. The pleiotropic effects of mutations in *ATM* and *Atm* indicate that these genes are involved in the proper functioning of a variety of mitotic, postmitotic and meiotically active cells.

Most AT patients (Boder, 1975; Sedgewick and Boder, 1991), and all *Atm*-deficient mice, of both sexes are infertile due to complete absence of mature gametes in adult gonads (Barlow et al., 1996; Elson et al., 1996; Xu et al., 1996). The seminiferous tubules of mutant males contain spermatogonia and Sertoli cells, but no normal spermatocytes, and display a complete absence of spermatids or mature sperm. In female mutants, the adult ovary

is devoid of maturing follicles, primordial follicles and oocytes. The severe nature of these defects in both sexes suggests that *Atm* is important during an early stage in meiosis I, possibly during meiotic prophase. This hypothesis is consistent with the meiotic recombination phenotypes of the *Atm* homologues *MEC1 (ESR1)* in *Saccharomyces cerevisiae* (Kato and Ogawa, 1994) and *mei41* in *Drosophila melanogaster* (Baker and Carpenter, 1972), and the meiotic checkpoint function of *MEC1* (Lydall et al., 1996). In addition, surface spread spermatocytes from *Atm*-deficient mice show abnormalities that suggest arrest in zygonema/pachynema of prophase I, with chromosome fragmentation (Xu et al., 1996; Plug et al., 1997). These results are consistent with an important role for *Atm* in prophase I of meiosis.

In support of the hypothesis that *Atm* plays an important role in meiotic prophase, we have recently demonstrated that RAD51 foci are not assembled properly on unpaired axial elements in leptotene of spermatocytes from *Atm*-deficient mice, and p53, p21 and BAX are elevated in mutant testes (Barlow et al., 1997a). In *Atm/p53* or *Atm/p21* double mutants, spermatogenesis progresses further into pachytene stages, but not to diplotene. Assembly of Rad51 foci on axial elements remains defective, and p53, p21 and BAX remain elevated unless genetically eliminated. These results demonstrate that *Atm* is important for proper RAD51 assembly onto the axial elements, as well as for suppressing p53, p21 and BAX levels in testes.

We have examined the infertility phenotype of *Atm*-deficient mice in detail in order to understand the role of *Atm* in meiosis and provide insight into the general function of this gene in cellular processes in vivo. We have analyzed the development of the germ cell defects in male and female gametogenesis, and performed morphological and fluorescent immunostaining analyses of meiosis in the adult testis using sections and surface spreads of spermatocytes. Our results indicate a crucial role for *Atm* as early as leptonema of prophase I during meiosis.

MATERIALS AND METHODS

Mating and genotyping mice

The construction of the *Atm*-deficient mice (allele designation $Atm^{ins5790neo}$) was previously described (Barlow et al., 1996). Mice from heterozygous crosses were genotyped by Southern blotting as described (Barlow et al., 1996), using *Eco*RV-digested DNA and a genomic probe surrounding the targeted exon, or by PCR (developed by Mai-Jing Liao and Terry Van Dyke). PCR primers are: ATM-F: GAC TTC TGT CAG ATG TTG CTG CC; ATM-B: CGA ATT TGC AGG AGT TGC TGA G; ATM-NEO: GGG TGG GAT TAG ATA AAT GCC TG. The PCR products are 440 bp for the mutant allele and 162 bp for the wild-type allele. Heterozygotes were derived from mating in a completely inbred 129SvEv background, or in a 129SvEv×NIH Black Swiss mixed background. No significant differences were observed between backgrounds (data not shown).

Histological analysis

Testes and ovaries were isolated and fixed in 20 volumes of 10% buffered formalin. Fixed tissues were embedded in paraffin or plastic, sectioned and stained using standard methods (Luna, 1992). Plastic sections of 1.8 μm in thickness were stained with toluidine blue. Sections were examined and photographed with light microscopy. For TUNEL assays, paraffin-embedded sections were dewaxed and analyzed using the TACS in situ kit (Trevigen).

Preparation of male meiotic prophase spermatocytes

Spreads of cells in meiotic prophase were prepared by the surface microspreading technique (Dresser and Moses, 1979) to allow sequential analysis of microspreads by light and transmission electron microscopy. In brief, a single cell suspension was prepared from testes of 2-month-old male mice. Cells were lysed in hypotonic salt (140 mM, pH 8.0) and nuclei attached to glass- or plastic-coated microscope slides. Nuclei were fixed for 6 minutes (2% paraformaldehyde, with or without 0.03% SDS, pH 8.2). After several washes with Photoflo (0.4% Kodak Photoflo 600 in distilled water, pH 8.2), slides were dried. Slides were stained for approximately 90 minutes at 60°C with a silver staining solution (50% silver nitrate, 0.03% formalin in distilled water). After destaining in distilled water, slides were air dried. Photographic images at the light microscopy level were acquired using a 100× objective.

For electron microscopy, slides were immersed in 30-50% silver nitrate, covered with nylon mesh and incubated in a moist environment for 10-30 minutes. Slides were then washed with Photoflo and the film containing the nuclei was floated off of the microscope slides onto the surface of distilled water. Grids were randomly placed on the film and the film with grids were lifted from the water surface by Parafilm. Isolated grids were examined by transmission electron microscopy and electron micrographs acquired at magnifications between 3,000 and 15,000×.

Immunohistochemistry

Paraffin-embedded tissues were prepared and used for immunohistochemistry according to standard techniques (Harlow and Lane, 1988), using the Renaissance TSA (Tyramide Signal Amplification, DuPont NEN, Boston, MA) kit for the enhancement of the fluorescent signal.

Fluorescence immunostaining of spread meiotic nuclei

Immunostaining of surface spreads of spermatocytes was performed as previously described (Dobson et al., 1994). Mouse anti-Cor1 and mouse anti-Syn1 antibodies were used as previously described (Dobson et al., 1994). Secondary antibodies were conjugated with FITC or rhodamine, and purchased commercially (Pierce).

Anti-ATM, ATR, DMC1 and RAD51 antibodies

Eight different antibodies to human and murine ATM, produced by several different laboratories, were used for immunohistochemistry and fluorescence immunostaining: two different lots of the anti-human ATM peptide (amino acids 1353-1366) antibody ATM-1 (or DH-1) from Oncogene Research (Cambridge, MA), which reportedly localized to the synaptonemal complexes (Keegan et al., 1996); two other anti-human ATM peptide antibodies from Oncogene Research (ATM-3: amino acids 13-24; and ATM-6: amino acids 819-844); two polyclonal anti-human ATM antibodies, generated from histidine-tagged fusion proteins spanning amino acids 1391-1693 (Atm.B) or amino acids 1980-1338 (Atm.V), which detect mouse ATM by immunoblot analysis (Lakin et al., 1996); a monoclonal anti-human ATM antibody (2C6), generated from a GST-fusion protein to amino acids 2577-3056, that also recognizes mouse ATM by immunoblot analysis (Barlow et al., 1997b; Chen and Lee, 1996); and pAb354, an anti-human ATM GST fusion protein antibody to amino acids 2287-2572 (K. B. and D. T., unpublished). Specific ATM localization was confirmed by comparing immunolocalization signals in wild-type and $Atm^{-/-}$ spermatocytes, since the 350 kDa ATM protein is not present in $Atm^{-/-}$ mouse tissues (Barlow et al., 1997b).

Two anti-human ATR antibodies were used for fluorescence immunolocalization studies: ATR-A and ATR-C (S. R. and S. P. J., unpublished data). Neither preimmune serum produces immunofluorescent foci on surface spermatocytes but ATR-A preimmune serum has a weak reaction with synaptonemal complexes, which is common for rabbit serum. The anti-mouse DMC1 antibody 17RTB is a mouse polyclonal antiserum (P. B. M. and M. T.,

unpublished) against His-tagged DMC1 that was expressed in bacteria from full-length mouse cDNA (Yoshida et al., 1998). All mouse preimmune sera were negative for meiotic prophase proteins. Before injection, the protein was purified on a Ni-NTA column. To eliminate cross-hybridization with RAD51, 17RTB was passed twice over a column containing RAD51 protein so that the elutriate recognized only DMC1 and not RAD51 by western blotting (data not shown). The anti-mouse RAD51 antibody was used as described (Dobson et al., 1994; Barlow et al., 1997).

RESULTS

Development of gametogenesis defects in *Atm*-deficient mice

We analyzed the developmental onset of the gametogenesis defects in *Atm*-deficient mice of both sexes. Primordial germ cells migrate from the allantois to the genital ridges by 11.5 days postconception (d.p.c.) (Hogan et al., 1994). Embryos from heterozygous crosses were fixed at 12.5 d.p.c., stained with alkaline phosphatase to detect germ cells in the genital ridges and genotyped by Southern analysis. Embryos of all three genotypes had equivalent numbers of alkaline phosphatase-positive germ cells in the genital ridges (data not shown), demonstrating that germ cell survival and migration to the ridges were unaffected in mutant mice.

Oocytes arrest in the postpachytene dictyate stage of meiosis I beginning late in gestation, and by 5 days after birth, all oocytes are arrested at this stage (Hogan et al., 1994). We examined the ovaries from wild-type and *Atm*-deficient embryos at embryonic day 16.5. Ovaries from wild-type mice had several primordial oocytes (Fig. 1A), as did ovaries from mutant mice (Fig. 1B). However, several oocytes in ovaries from mutant mice appeared to be undergoing apoptotic degeneration and had pycnotic nuclei (Fig. 1B, inset). These observations were confirmed by the TUNEL in situ assay for apoptosis. TUNEL-positive oocytes were rarely observed in ovaries from wild-type mice (Fig. 1C), but there were many TUNEL-positive oocytes in ovaries from mutant mice (Fig. 1D, and inset) demonstrating that oocytes degenerated prior to birth in *Atm*-deficient mice. After birth, in wild-type mice, oocytes continue to mature until recruited at and after puberty for progression to mature follicles. Wild-type ovaries at 11 days of age (Fig. 1E) were filled with oocytes, primordial follicles and maturing follicles (see inset). However, ovaries from *Atm*-deficient mice at 11 days (Fig. 1F) were devoid of oocytes and follicles (Fig. 1F, inset). Only one ovary out of eight examined had any follicles at all, and in this case only a single abnormal follicle was observed (data not shown).

As we previously showed (Barlow et al., 1996), adult ovaries from mutant mice were barren, without any oocytes. In addition, attempted superovulation of several mutant females did not lead to follicle formation (data not shown), supporting the observation that mutant ovaries contained no oocytes. These results demonstrate that the defect in oogenesis in *Atm*-deficient mice is complete and occurs prior to or during the dictyate stage of prophase I arrest.

Soon after arriving in the gonadal ridge, male prospermatogonia undergo arrest (reviewed in Bellvé, 1993). After birth, the spermatogonia divide mitotically. These type A spermatogonia populate the seminiferous tubules and thereafter reside adjacent to the basement membrane. Testes from wild-type (Fig. 2A) and *Atm*-deficient mice (Fig. 2B) were indistinguishable at 8 days of age, demonstrating that normal differentiation and mitotic division of spermatogonia occur in the absence of *Atm*. Between 8 and 10 days of age, some type A spermatogonia differentiate to type B spermatogonia, which then progress into meiotic prophase as spermatocytes. By 16 days of age, leptotene, zygotene and pachytene spermatocytes can be identified. Testis from 16-day-old wild-type mice (Fig. 2C) contained all of these cell types. In contrast, normal spermatogenesis was completely disrupted in *Atm*-deficient mice (Fig. 2D). Spermatogonia and Sertoli cells were present along the basement membrane, but no normal spermatocytes could be identified. Instead, there were smaller, pycnotic cells that appeared to be undergoing apoptotic degeneration. These observations were confirmed by the TUNEL in situ assay. Seminiferous tubules from wild-type controls had only low numbers of TUNEL-positive cells (Fig. 2E). However, there was a four-fold increase in apoptotic, degenerating cells in tubules from *Atm*-deficient littermates (Fig. 2F).

We previously showed (Barlow et al., 1996) that sections from adult testes of *Atm*-deficient mice contained only

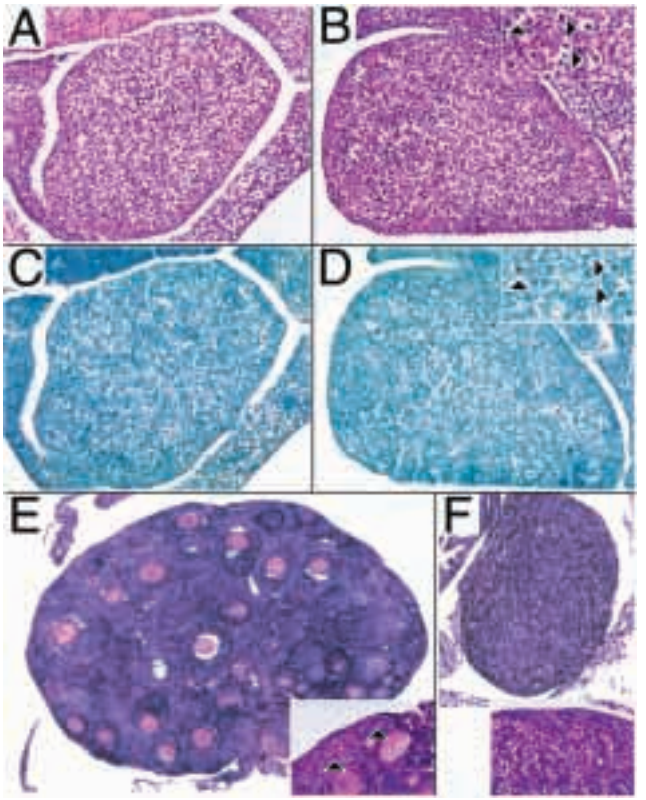

Fig. 1. Abnormal oogenesis in *Atm*-deficient mice. Embryonic day 17.5 ovaries from wild-type (A) and mutant (B) littermates stained with hematoxylin and eosin. Note the pycnotic cells in the ovary from mutant mice (B, inset, arrowheads). Wild-type (C) and mutant (D) ovaries were examined for apoptotic cells by the TUNEL in situ assay and positive cells were only detected in the mutant ovary (D, inset, arrowheads). (C,D) Adjacent sections to A and B, respectively. Hematoxylin and eosin stained sections of ovaries from 11-day-old wild-type (E) and mutant (F) mice. The arrowheads indicate primary oocytes in preantral follicles. Magnifications were 20× (E,F), 40× (A-D) and 60× (insets).

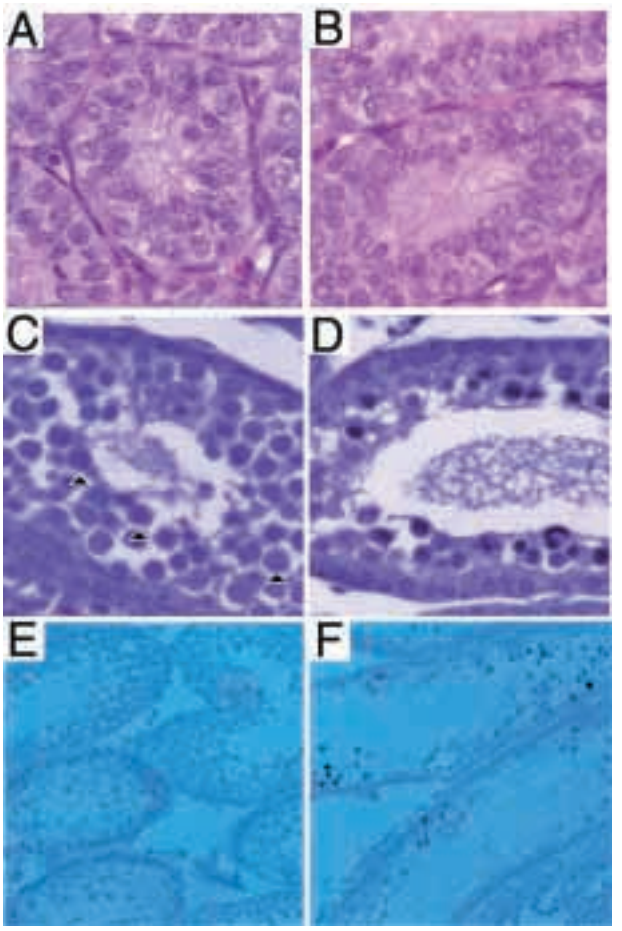

Fig. 2. Abnormal spermatocyte development in *Atm*-deficient mice. Hematoxylin and eosin stained sections of mouse testes from 8-day-old wild-type (A) and mutant (B) mice are similar. By day 16.5 of age, toluidine blue staining of testes sections demonstrates the presence of disrupted spermatogenesis and degenerating cells in the mutant (D) as compared to the normal mouse (C). Arrowheads indicate normal pachytene spermatocytes present in wild-type (C), but absent in mutant (D) mice. TUNEL assay demonstrates an increase in apoptotic cells in the 16.5-day-old mutant (F) as compared to the normal mouse (E). A-D are 100× magnification; E,F are 40× magnification.

spermatogonia, abnormal spermatocytes and degenerating cells, as well as Sertoli and Leydig cells (data not shown). We have never seen any form of spermatid or maturing spermatozoa, demonstrating that the defect in meiosis is complete and profound. The developmental defects of both oogenesis and spermatogenesis observed in *Atm*-deficient mice demonstrate that there is a total disruption of meiosis during prophase I. Neither oocytes nor normal spermatocytes were present during any stage of development, demonstrating that *Atm* plays an essential role in prophase of meiosis I.

Electron microscopic analysis of *Atm*-deficient spermatocytes

To identify meiotic defects in cells from *Atm*-deficient mice, we examined silver-stained microspreads from wild-type and mutant mice by light (data not shown) and electron microscopy. In wild-type mice, all stages of prophase I were observed (data not shown). In microspreads from *Atm*-deficient mice, however, normal prophase I stages were rarely observed (Fig. 3). Defects in the axial elements were widespread in mutant spreads (Fig. 3A,B), synaptonemal complexes displayed abnormal, non-homologous pairing (Fig. 3C,D, arrow), and there were small, paired and unpaired synaptonemal complex fragments observed in many spreads (Fig. 3B-D, arrows).

At higher magnification, normal chromosomal pairing and synapsis occurred in some regions of synaptonemal complexes, but extensive pairing abnormalities with discontinuities were observed in several complexes (Fig. 3E, arrowhead). These axial gaps, occurring on a single axis of the paired synaptonemal complex, were often found and were approximately 10-25% of the length of the complex. Axial gaps were found located in the middle or end of the synaptonemal complex. In microspreads that contained complexes with axial gaps, fragments of what appeared to be a single axis and fragmented termini were often observed (data not shown). These abnormalities were not observed in spermatocytes from wild-type mice (data not shown).

In many spreads from mutant mice, fragmentation was more extensive, resulting in complete disruption of all synaptonemal complexes (Fig. 3F). It is not clear whether the fragmented complexes represented apoptotic cells, or a stage intermediate between axial gap formation and apoptosis. In either case, no normal spermatocyte spreads were observed in the mutant mice after axial pairing. These results demonstrate that the loss of *Atm* results in a severe and complete disruption of meiosis I, and the end result is chromosomal fragmentation and apoptosis.

Prophase I disruption in *Atm*-deficient spermatocytes

To define the meiotic defect in *Atm*-deficient mice more precisely, we compared meiotic prophase stages in microspreads of spermatocytes from wild-type and *Atm* mutant littermates immunostained for chromosome cores, centromeres and ATR protein, a closely related family member of ATM (Fig. 4). Staging was based on three criteria: traditional meiotic chromosome morphology; centromere configuration (single versus paired); and ATR immunofluorescent foci patterns. In agreement with previously published data (Keegan et al., 1996), we found that ATR was predominantly localized to the unpaired axial elements of the developing synaptonemal complexes between leptonema and pachynema (Figs 4, 5A-C), although there was some localization to paired axial elements. In mid-to-late pachynema, the rare unpaired axial regions stain brightly with ATR (Fig. 5A, arrows). ATR was not found in association with chromatin in wild-type spermatocyte spreads. Thus, ATR is a marker of early prophase I axial element assembly.

Leptonema

Short segments of chromosome cores have started to form in microspread nuclei of this stage from wild-type testes (Fig. 4A). There was no evidence for synapsis and there were 40 bright fluorescent centromeres. ATR foci were evenly distributed over the chromosome core segments (Fig. 4B). The sperm tails and nuclei in the background serve as evidence that spermatogenesis was efficient in this wild-type mouse. In leptotene nuclei from an *Atm*-deficient littermate (Fig. 4C,D), the short chromosome core segments and the 40 single centromeres were similar in

appearance to the wild type, but the ATR pattern was disturbed. Instead of the regular distribution of foci seen in the wild type, there were conspicuous clusters of bright ATR foci. Examining a large number (50+) of such nuclei, it was evident that there was a range of abnormalities (see Fig. 7). Some mutant leptonema nuclei had a pattern of ATR localization that was similar to the wild-type control and some had greater aggregations of foci than shown here (see Fig. 5). Thus, abnormalities of spermatogenesis were detectable as early as leptonema in *Atm*-deficient spermatocytes.

Zygonema

In microspread nuclei of this stage from *Atm* wild-type testes (Fig. 4E), when core formation was still in progress, homologs initiated intimate synapsis as judged by synaptonemal complex formation. In the nucleus shown, nine pairs of centromeres had completed synapsis and there were 22 unpaired centromeres. ATR foci (Fig. 4F) were brightest on unpaired and recently paired cores, and the X-Y pair was not distinguishable at this time. There were no aggregates of foci of the type seen in zygotene spermatocytes of mutant mice. In mutant nuclei of this stage (Fig. 4G), the appearance of single cores, partially paired cores and mature synaptonemal complexes was typical for the zygotene stage of meiosis. There were 14 sets of paired and 12 single centromeres. From these two parameters alone, it would be difficult to differentiate zygonema between wild-type and mutant spermatocytes. However, there was abnormal aggregation of ATR antigen in mutant nuclei, as described for leptonema. This abnormality varied from mild (Fig. 4H), to heavy aggregations throughout the nucleus.

Pachynema

The standard karyotype of this stage from wild-type spermatocytes had 19 bivalents and the X-Y pair (Fig. 4I). The X and Y chromosome cores were strongly stained with the ATR antibody and the entire sex vesicle was reactive as well (Fig. 4J). However, we have only rarely seen such normal pachytene images in mutant spermatocytes. Invariably, segments of single cores, unpaired centromeres and misaligned centromeres were observed (Fig. 4K). The Atr foci were less intense, as in the wild type, but the X-Y pair had not accumulated ATR antigen in mutant spermatocytes (Fig. 4L).

Diplonema

In spreads from wild-type mice, homologous chromosomes and their cores started to repel each other (Fig. 4M), while the ATR signal from the X-Y and sex vesicle faded (Fig. 4N). No normal diplotene was observed in mutant spermatocytes (Fig. 4O). The major phenotype displayed was the breakup of chromosome cores. It might be argued that this is an early meiotic prophase stage but the lack of ATR foci eliminated that possibility (Fig. 4P). As was the case for pachynema in the mutant, the X-Y pair was not differentiated by ATR fluorescence.

ATR, DMC1 and RAD51 fluorescent immunostaining of surface spreads

We performed immunostaining of surface spreads using antibodies that detect proteins that associate with the developing synaptonemal complex at various stages of prophase I, beginning in leptonema. We examined the localization of ATR, DMC1 and RAD51.

As described above, we found that ATR was predominantly localized to the unpaired axial elements of the developing synaptonemal complexes between leptonema and pachynema (Figs 4, 5A-C), although there was some localization to paired axial elements. In mid-to-late pachynema, the rare unpaired axial regions stain brightly with ATR (Fig. 5A arrows). ATR was not found in association with chromatin in wild-type spermatocyte spreads. In contrast, in microspreads from *Atm*-deficient mice, there was a reduction in axial element-associated ATR and a substantial fraction of ATR was now associated with chromatin (Fig. 5D-F). In addition, as described above (Fig. 4),

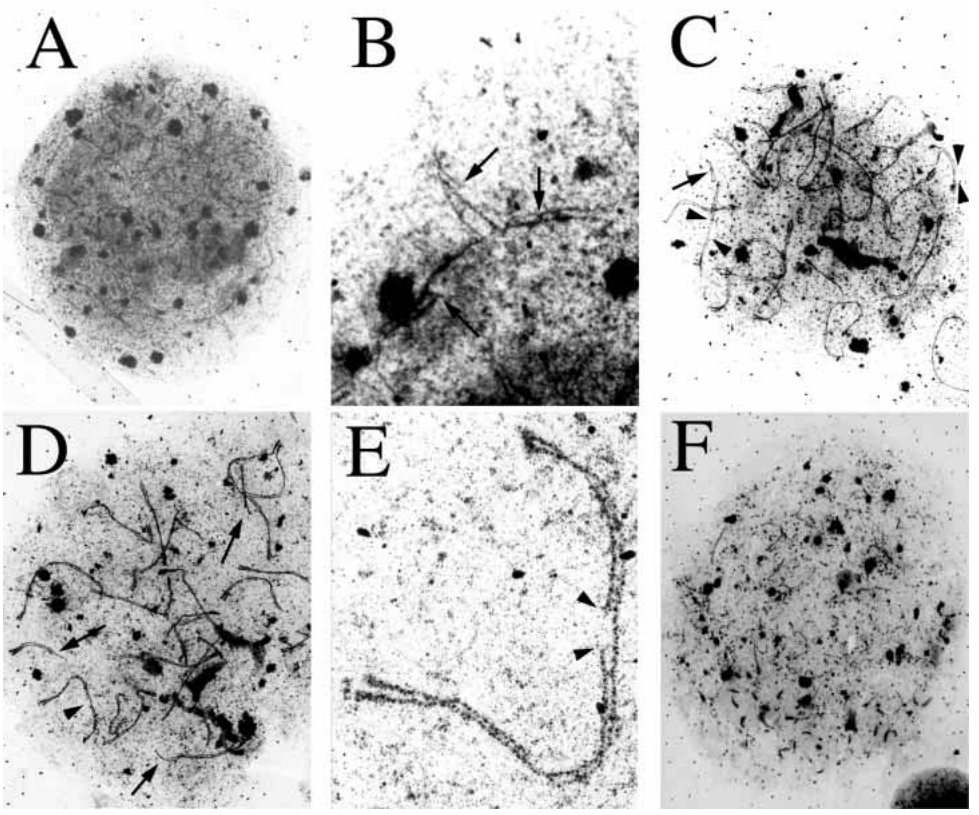

Fig. 3. Examination of synaptonemal complexes by transmission electron microscopy in silver-stained prophase microspreads of spermatocytes from *Atm*-deficient mice. Low (A,C,D,F) and higher (B,E) magnification views of synaptonemal complexes from mutant early spermatocytes are shown. Note the unpaired axes (B-D, arrows) and an axial gap (C-E, arrowhead) in a complex from the *Atm*-deficient spermatocyte. Magnifications: (A) 2000×; (B) 8000×; (C,D,F) 3000×; (E) 12,000×.

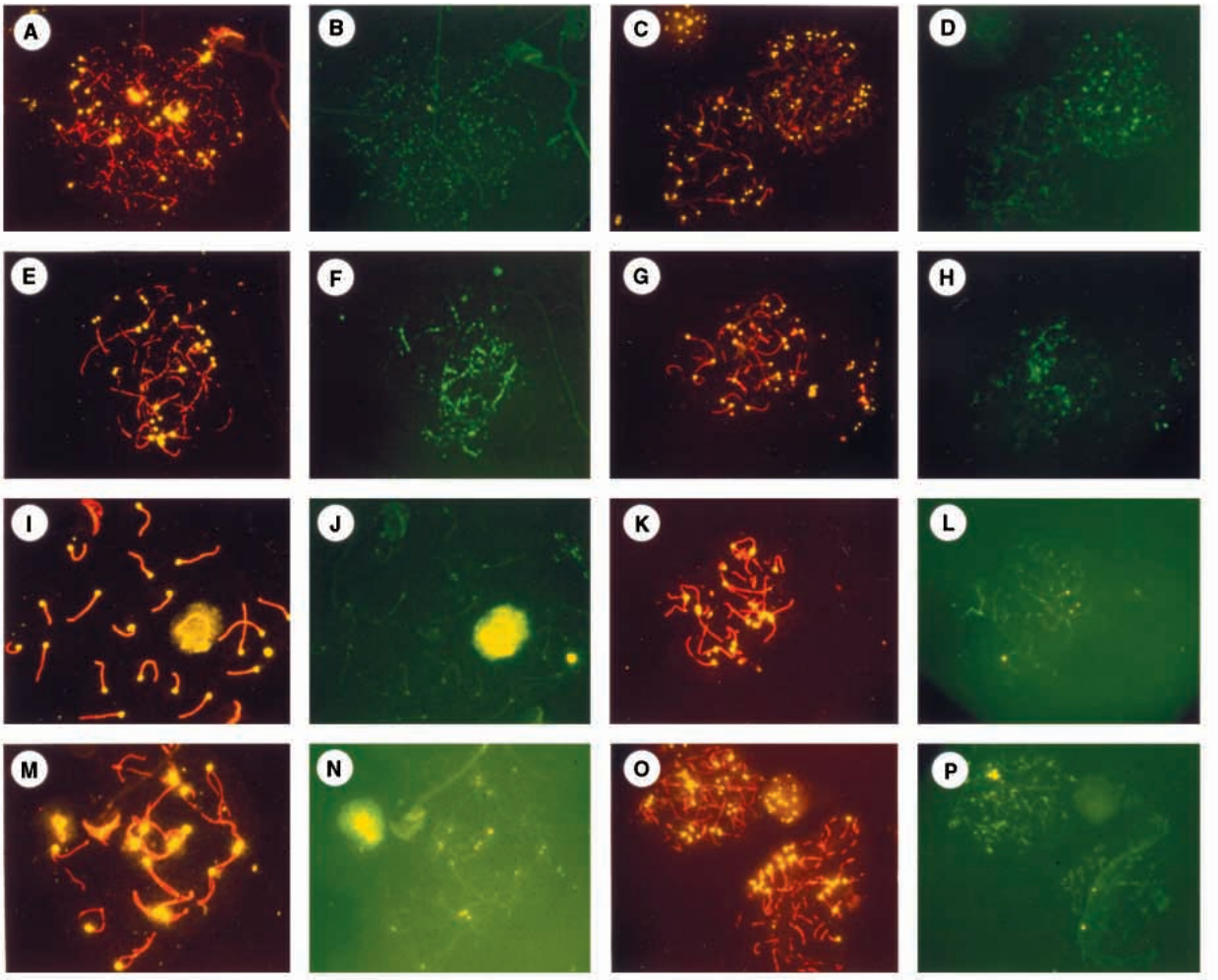

Fig. 4. Immunofluorescent meiotic prophase staging of wild-type and *Atm*-deficient mouse spermatocytes based on core/synaptonemal complex morphology (red) centromere behaviour (yellow) and ATR antigen distribution (green). (A,B,E,F,I,J,M,N) Wild type; (C,D,G,H,K,L,O,P) mutant; (A-D) leptonema; (E-H) zygonema; (I-L) pachynema; (M-P) diplonema.

there was an abnormal overload of ATR on unpaired segments of mutant spreads, seen as bright spots on asynapsed complexes (Fig. 5E, arrow and scattered throughout the nucleus of the spermatocyte in the bottom right of the panel).

Two recA homologs, DMC1 and RAD51, are present on axial elements of the developing synaptonemal complexes in early prophase I of meiosis in *Saccharomyces cerevisiae* (Bishop et al., 1992; Bishop, 1994). Murine DMC1 (Yoshida et al., 1998) and Rad51 (Moens et al., 1997) are detected in leptotene and zygotene spermatocytes. We examined the pattern of localization of mouse DMC1 and RAD51 in microspread preparations of spermatocytes from wild-type and *Atm*-deficient mice, using purified antibodies that do not cross-react with each other. DMC1 was predominantly localized to the developing synaptonemal complexes (Fig. 6A), as shown in a more careful analysis of this pattern of localization (P. B. M., M. T., T. Morita and B. Spyropoulos, unpublished data). In microspreads from *Atm*-deficient mice, there was a reduction in axial element-associated DMC1 and a substantial fraction was now associated with chromatin (Fig. 6B,C).

RAD51 is localized to unpaired axial elements and paired synaptonemal complexes in association with Cor1 during leptonema and zygonema, and disappears from all but the unpaired X chromosome in pachynema (Moens et al., 1997 and Fig. 6D). In comparison, RAD51 mislocalization can be detected in leptotene spermatocytes from *Atm*-deficient mice (Fig. 6E), as we reported previously (Barlow et al., 1997a). Thus, ATR, DMC1 and RAD51, markers of early prophase I axial element assembly, were abnormal in their localization in *Atm*-deficient mice, consistent with the severe disruption of meiosis during early prophase I in mutant mice.

Although most mutant spermatocytes displayed abnormal localization of these three synaptonemal complex proteins, occasional mutant spermatocytes with near normal RAD51 (Fig. 6F), ATR (Fig. 5E, spermatocyte in the upper right of the panel) or DMC1 (Fig. 6C, spermatocyte on the left side of the panel) localization could be observed. To quantify the degree to which spermatogenesis was disrupted in *Atm*-deficient mice, we scored the number of spermatocytes that had normal or near-normal morphology as compared to those that were grossly abnormal after staining with anti-ATR (Fig. 7A) or anti-DMC1 (Fig. 7B), in addition to anti-centromere and anti-Cor1 antibodies. Using anti-ATR, a few spermatocytes had near-normal early leptotene morphology, but many were abnormal

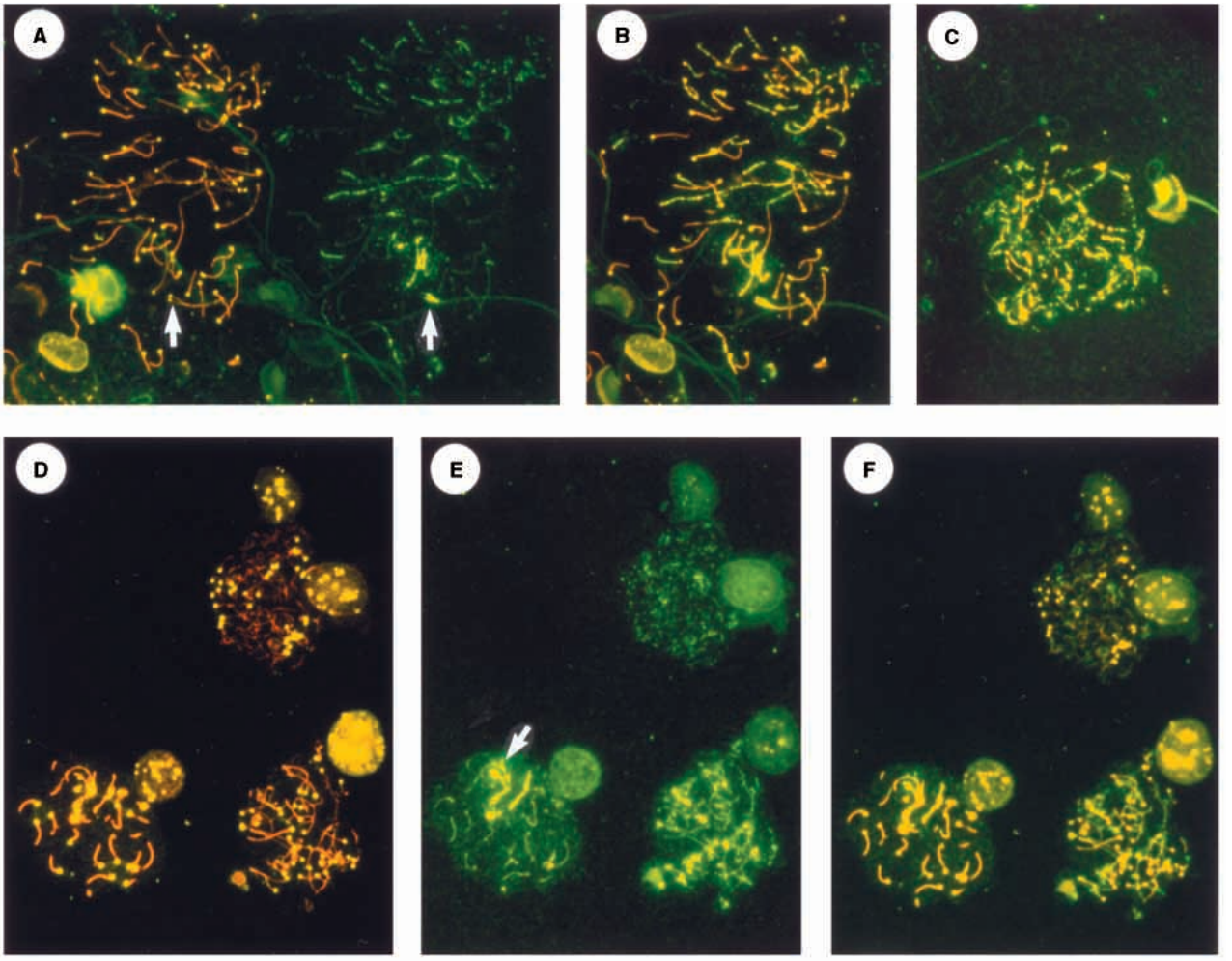

Fig. 5. ATR localization in wild-type and *Atm*-deficient mice. (A, left) Wild-type zygotene synaptonemal complexes using a mixture of Cor1 and Syn1 (orange); (A, right) the same complexes after staining with anti-ATR (green). Arrows indicate that rare unpaired axial regions stain brightly with ATR. (B) These two panels are overlaid. (C) A second example of wild-type colocalization of Cor1/Syn and ATR. (D-F) Three different spermatocyte stages in spreads from *Atm*-deficient mice (although spermatocytes are not completely normal): leptonema in the upper cell, zygonema in the lower right cell and pachynema in lower left cell. The synaptonemal complexes, stained with (D) Cor1/Syn1 mixture (yellow); (E) ATR (green) and (F) an overlay of D and E, displayed some ATR staining localized to synaptonemal complexes (arrowhead) but in others there was lack of colocalization.

at this stage. In addition, the localization of DMC1 is abnormal in the majority of cells by mid-zygonema and pachynema, and ATR localization is almost completely abnormal in zygonema. These data are consistent with observations by electron microscopy, suggesting that meiosis becomes abnormal in *Atm*-deficient spermatocytes as early as leptonema.

Immunolocalization of ATM in gonadal sections

We determined the localization of ATM in ovaries and testes, using anti-ATM antibody pAb354. In ovaries of wild-type mice, murine ATM was predominantly localized in the cytoplasm of ova in developing ovarian follicles (Fig. 8A,B). Minimal nuclear staining was detected. No ATM signal was detected in ovaries from *Atm*-deficient mice (data not shown), which are devoid of oocytes and developing follicles.

Several antibodies displayed a similar nuclear staining pattern in testes sections of wild-type mice, including pAb354 antibody (Fig. 8C,D), the monoclonal antibody 2C6 (Barlow et al., 1997b; Chen and Lee, 1996), and ATM-3 and ATM-6 from Oncogene Research (data not shown). The staining pattern was diffuse, usually in cells near the periphery of the seminiferous tubules, consistent with ATM localization in spermatogonia (Fig. 8D). However, we did observe ATM staining in more centrally located cells in seminiferous tubules. Occasionally, these centrally located cells containing ATM also stained with Cor1 (data not shown), so were probably meiotic spermatocytes. This pattern was absent in sections from $Atm^{-/-}$ spermatocytes using antibody pAb354 (Fig. 8E,F) or several other antibodies (data not shown), demonstrating that this signal represents ATM protein. Other antibodies, such as ATM-1 (or Ab-1, DH-1 from Oncogene Research), used in previous immunolocalization studies (Keegan et al., 1996; Plug et al., 1997), displayed a very weak signal in sections from wild-type testes (data not shown). Thus, ATM is located in cells within male and female gonads that are either prepared to enter or have entered meiosis.

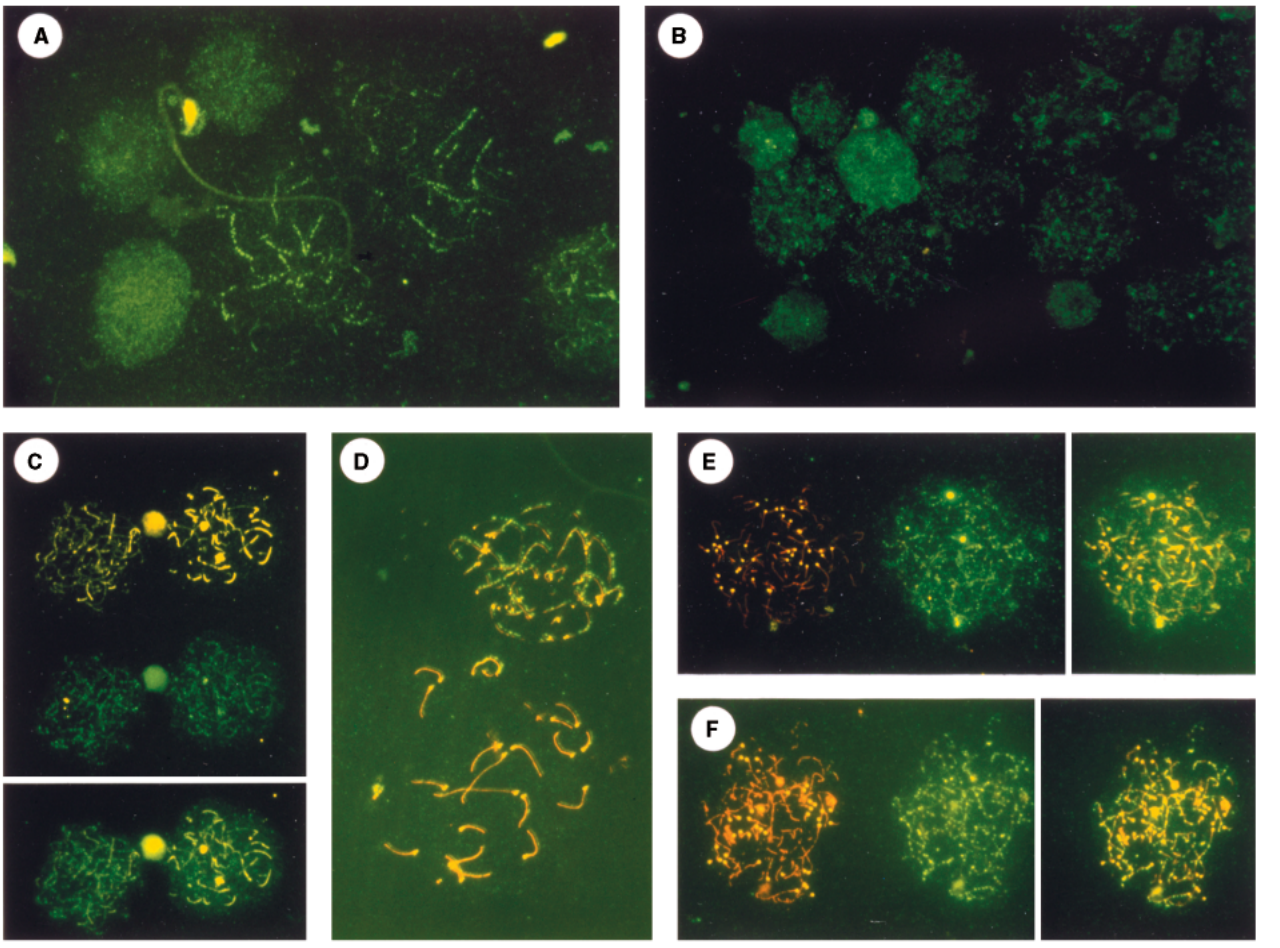

Fig. 6. DMC1 and RAD51 localization in wild-type and *Atm*-deficient mice. DMC1 staining of wild-type (A) and *Atm*-deficient (B,C) spermatocytes are shown. RAD51 staining of wild-type (D) and *Atm*-deficient (E,F) spermatocytes are shown.

ATM fluorescent immunostaining of surface spreads of spermatocytes

It has been reported that ATM localizes to the paired axes of the synaptonemal complex during zygotene and pachytene stages of meiotic prophase I, using antibody ATM1 (Keegan et al., 1996; Plug et al., 1997). We have used several ATM antibodies, including ATM1, to determine the pattern of localization of murine ATM in microspreads of spermatocyte nuclei.

Using antibody pAb354, a weak but noticable chromatin-associated pattern of ATM was observed in wild-type spermatocyte nuclei. At 1:1000 dilution of this antibody, ATM was strongest in nuclei of spermatogonia (Fig. 8G), and some weak foci of ATM were associated with the synaptonemal complex as well as chromatin. However, these were at much lower intensities than the strong, nuclear spermatogonial signal. The same patterns were also observed in microspreads from *Atm*-deficient mice (Fig. 8H), suggesting that they represent non-specific binding in spermatocyte surface spreads.

We found, using two batches of the ATM-1 antibody (David Hill, Oncogene Research) at high concentration (1:50 dilution), that this antibody also bound in a diffuse pattern to chromatin in meiotic spreads from wild-type mice, with very little localization to unpaired or paired axial elements, and the identical staining pattern was seen in *Atm*-deficient mice (data not shown). None of the other anti-ATM antibodies displayed specific binding to unpaired or paired axial elements of the developing synaptonemal complex of mouse, but instead were bound diffusely to chromatin (data not shown). These results suggest that this diffuse nuclear localization pattern may reflect the presence of ATM in meiotic nuclei, consistent with the immunolocalization studies described above. However, we have found no evidence for specific synaptonemal complex localization of ATM protein. In addition, these results also suggest that ATM antibodies cross-react with other epitopes in spermatocyte spreads, but that these epitopes are not recognized by these antibodies when applied to tissue sections.

DISCUSSION

The infertility phenotypes of AT patients (Boder, 1975; Sedgewick and Boder, 1991) and *Atm*-deficient mice (Barlow et al., 1996) are consistent with an important role for *ATM* and *Atm* in meiosis. We have characterized the severe and complete gametogenesis defects that occur in *Atm*-deficient mice, and have found that meiosis is disrupted in males and females early in prophase I. *Atm* is not required for germ cell migration in embryogenesis. In addition, *Atm* is not required for mitotic division of spermatogonia or oogonia, nor is it necessary for entry into meiosis. However, ovaries were devoid of oocytes prior to dictyate arrest due to degeneration and apoptosis of

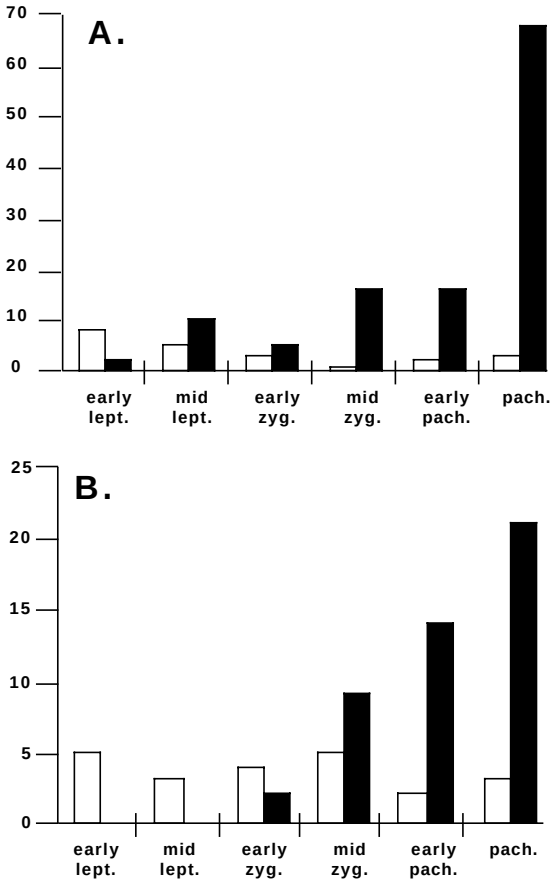

Fig. 7. Quantitation of normal and abnormal prophase I spermatocytes in *Atm*-deficient mice, using spreads from immunolocalization studies of anti-ATR (A) and anti-DMC1 (B).

germ cells, and normal spermatogenesis progressed only to the initiation of meiosis I. Analysis of male meiosis in microspreads of prophase I spermatocytes from *Atm*-deficient mice demonstrated that the integrity of the axial elements and synaptonemal complexes was disrupted. Axial gaps in the paired synaptonemal complexes were identified as early as paired axes could be identified, followed by complete disruption of meiosis with chromosomal fragmentation and apoptosis of spermatocytes.

Analysis of the expression pattern of ATM protein in testes and ovary was consistent with an important role in early meiosis. Expression was highest in the ovarian follicles and in testicular spermatogonia. In microspreads of spermatocytes, ATM did not appear to be associated with axial elements of the developing synaptonemal complex. We examined the localization of a closely related ATM family member, ATR (Keegan et al., 1996), and the recA homologs DMC1 and RAD51 in spermatocyte spreads. We found that axial element association of these proteins was reduced in spermatocytes from *Atm*-deficient mice, and that they were mislocalized to chromatin, suggesting that meiosis was disrupted prior to pachytene. In support of this, *Dmc1*-deficient mice display defects in homologous chromosome synapsis and arrest in zygotene stages of prophase I (Pittman et al., 1998; Yoshida et al., 1998). In addition, we quantified the number of abnormal spermatocyte nuclei in spreads stained with ATR and DMC1 and, in both cases, abnormal leptotene nuclei were detected (Fig. 7). These results support a role for ATM as early as leptonema.

Recently, we have shown that there is a similar reduction of axial element-associated RAD51 foci in spermatocytes from *Atm*-deficient mice, and that a substantial fraction of RAD51 was chromatin-associated as well (Barlow et al., 1997a). We repeated these findings in this manuscript, although the defects were less severe than previously reported. These findings suggested that meiosis was disrupted in the earliest stages of prophase I in *Atm*-deficient mice. We showed that p53, p21 and BAX were elevated in testes from *Atm*-deficient mice, and meiosis progressed further in double mutant mice with mutations in *Atm* and p53, or *Atm* and *p21* (Barlow et al., 1997a). Surprisingly, nearly normal pachytene synaptonemal complexes were observed in these double mutants. Thus, pachytene stages could be reached in the absence of *Atm*, demonstrating that *Atm* is not absolutely required for homologous pairing and synaptonemal complex formation. However, meiosis was arrested in the double mutants in pachytene stages, prior to diplotene, and further meiotic progression was not observed. In addition, defective RAD51 assembly was not rescued in the double mutants.

ATM may be directly required for the assembly of ATR, DMC1 and RAD51 on axial elements in preparation for meiotic recombination, perhaps by phosphorylation. Alternatively, ATM may be important for monitoring meiotic events that occur prior to ATR, DMC1 or RAD51 assembly onto the axial elements, to insure that the process is completed before assembly is attempted. In the first case, ATM would positively regulate protein assembly onto the developing synaptonemal complexes while, in the second case, ATM would be a negative regulator.

The cellular phenotype of mitotic cells from AT patients or *Atm*-deficient mice support the hypothesis that ATM plays a role in regulating cell cycle progression (Meyn, 1995; Shiloh, 1995). Radiation-induced G_1, M and G_2 checkpoints appear to function abnormally in cells from AT patients, and there is defective induction of p53, p21 and GADD45 (Artuso et al., 1995; Kastan et al., 1992). Cell cycle checkpoint defects, associated with defective p53 and p21 induction, have also been demonstrated in vivo in *Atm*-deficient mice after ionizing radiation (Barlow et al., 1997b). Finally, tail fibroblasts derived from *Atm*-deficient mice grow poorly and have cell cycle checkpoint abnormalities, as defined by radioresistant DNA synthesis (Barlow et al., 1996) and cell cycle analysis (Xu and Baltimore, 1996). These studies support the hypothesis that ATM is part of a signal transduction cascade regulating cell cycle progression, particularly after DNA damage.

ATM may perform similar functions in meiosis. Although DNA damage per se is not occurring in meiosis, DNA strand breaks occur during meiosis as a consequence of meiotic recombination. It is possible that progression through the multiple, intricate steps of meiosis are monitored and regulated similarly to cell cycle progression in mitosis, and that meiosis evolved from a mitotic cell cycle (Kleckner, 1996). Our results suggest that ATM participates in monitoring meiotic progression and, perhaps, meiotic recombination. ATM may perform similar functions in monitoring the progression of recombination in the thymus, during V(D)J recombination and T-cell maturation. V(D)J recombination most likely occurs in a

single phase of the cell cycle, namely G_1 (reviewed in Lin and Desiderio, 1995) yet, in the absence of ATM, thymic V(D)J recombination is disrupted, resulting in T-cell abnormalities and lymphoreticular malignancies (Barlow et al., 1996; Elson et al., 1996; Xu et al., 1996). Thus, ATM may serve as a mitotic cell cycle checkpoint, a monitor of V(D)J recombination, as well as a monitor of progression through meiotic recombination.

The mitotic and meiotic phenotypes of the *Atm* homologues *MEC1* and *mei41* support such a model. *MEC1* is an essential gene in yeast required for mitotic cell cycle checkpoint function (Weinert et al., 1994) and meiosis (Kato and Ogawa, 1994). *MEC1* functions as a meiosis I checkpoint during pachytene to ensure that meiotic recombination is complete before progressing to metaphase I (Lydall et al., 1996). If ATM acts as a regulator of meiotic progression, it must act at an earlier step in meiosis than *MEC1*. However, the *mec1-1* mutation, which was used to analyze the meiotic checkpoint function of *MEC1*, is a null mutation that is viable due to an unlinked suppressor (Lydall et al., 1996). This suppressor could potentially mask earlier checkpoint functions of *MEC1*. Similarly, *mei41* is required for normal frequency and distribution of meiotic recombination events (Baker and Carpenter, 1972), and mitotic checkpoint function (Hari et al., 1995) in *Drosophila*. In addition, the morphology of late recombination nodules is abnormal in *mei41* mutants (Carpenter, 1979), supporting a role for this *Atm* homolog in meiotic recombination.

A recent study reported that ATM localizes to zygotene and pachytene meiotic chromosomes along the paired axes of the synaptonemal complex, yet ATM was not seen on the unpaired axial cores in leptotenema and zygotenema (Keegan et al., 1996). Similar findings were presented in another paper from the same group (Plug et al., 1997). We have been unable to repeat the synaptonemal complex localization, using several different ATM antibodies, including the same antibody used in the above studies (Keegan et al., 1996; Plug et al., 1997). In addition, we have demonstrated that ATM function is required in leptonema. This suggests that the reported localization of ATM to the paired axes during zygotene and pachytene is inconsequential to the early meiotic defects that we have observed in *Atm*-deficient mice, since this localization occurs after the leptotene phenotype and RAD51 assembly defects. This does not preclude an additional role for ATM in later stages of prophase I. Our results, using several different antibodies on wild-type and *Atm*-deficient spermatocytes, suggest that the previously reported localization studies (Keegan et al., 1996; Plug et al., 1997) result from binding of the ATM-1 antibody to non-ATM proteins. The authors of the previous study did not test the specificity of the ATM1 antibody using spermatocyte spreads from *Atm*-deficient mice, as we have in this study. We have been unable to find any evidence for specific localization of ATM to the unpaired or paired axes of the developing synaptonemal complex in spermatocytes. Instead, immunolocalization studies with tissue sections from ovaries and testis and spermatocyte surface spreads are consistent with the interpretation that ATM is localized diffusely in nuclei of spermatogonia and early spermatocytes,

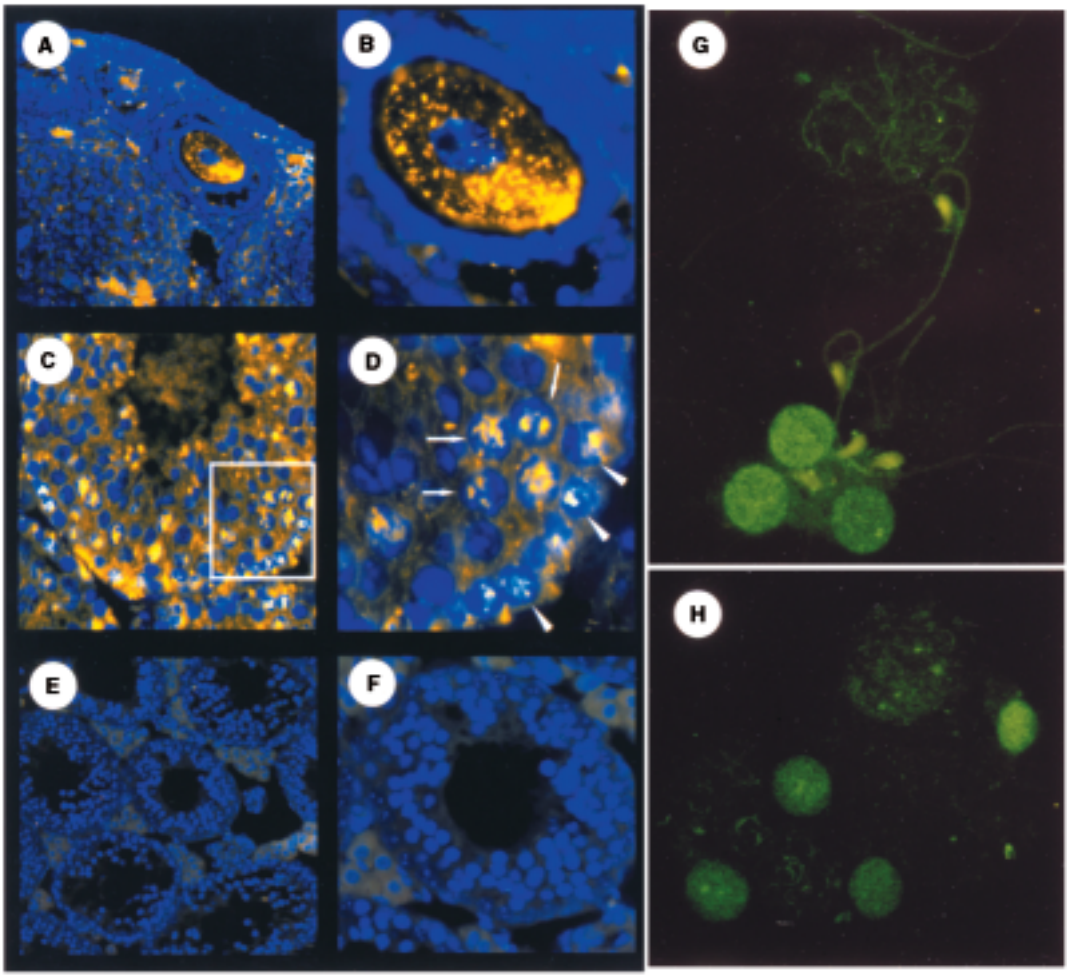

Fig. 8. Immunohistochemical localization of ATM in ovaries (A,B) and testes (C,D) from wild-type mice or in testes from *Atm*-deficient mice (E,F). The developing ovarian follicle in A (16×) is enlarged in B (100×). The area boxed in C (40×) is displayed at higher magnification in D (100×). Thin arrows indicate spermatocytes and arrowheads indicate spermatogonia. Similarly, the central seminiferous tubule in E (16×) is enlarged in F (40×). pAb354 was used at 1:200 and anti-rabbit-HRP at 1:500 dilution. Staining patterns of spermatocyte spreads using anti-ATM antibody pAb354 at 1:1000 dilution, in spermatocyte spreads from wild-type (G) and *Atm*-deficient (H) mice.

similar to the pattern observed in mitotic cells (Brown et al., 1997; Chen and Lee, 1996; Lakin et al., 1996).

The understanding of the mechanisms that control the early events of mammalian meiosis, especially the early stages of axial core formation, synaptonemal complex pairing and meiotic recombination, will likely result from the genetic analysis of mutants with phenotypes during these early events. The severe, early and profound defects in meiosis that we have described for the *Atm*-deficient mouse demonstrate that *Atm* plays a crucial role during prophase I. Thus, the *Atm*-deficient mice provide an excellent tool that can be used to further dissect early events in meiotic prophase I and meiotic recombination.

We would like to thank Matthew Gonda for assistance with early electron microscopy experiments, Doug Bishop for insight into meiosis and comments on the manuscript, Mike Dresser for helpful discussions about EM analysis of meiosis, Akira Shinohara for the Rad51 antibody, Darryl Leja for assistance in figure preparation, Mona Schröder, Denise Larson, and Lisa Garrett for excellent technical assistance, and Robert Nussbaum for generous support. C. B. is a Clinical Endocrine Fellow supported by the National Institute of Diabetes, Digestive, and Kidney Diseases, and P. B. M. was financially supported by the National Research Council of Canada.

REFERENCES

Artuso, M., Esteve, A., Bresil, H., Vuillaume, M. and Hall, J. (1995). The role of the Ataxia telangiectasia gene in the p53, WAF1/CIP1(p21)- and GADD45-mediated response to DNA damage produced by ionising radiation. *Oncogene* **11**, 1427-1435.

Baker, B. S. and Carpenter, A. T. C. (1972). Genetic analysis of sex chromosomal meiotic mutants in *Drosophila melanogaster*. *Genetics* **90**, 255-286.

Barlow, C., Hirotsune, S., Paylor, R., Liyanage, M., Eckhaus, M., Collins, F., Shiloh, Y., Crawley, J. N., Ried, T., Tagle, D. and Wynshaw-Boris, A. (1996). Atm-deficient mice: a paradigm of ataxia telangiectasia. *Cell* **86**, 159-171.

Barlow, C., Liyanage, M., Moens, P. B., Deng, C.-X., Ried, T. and Wynshaw-Boris, A. (1997a). Partial rescue of the severe prophase I defects of *Atm*-deficient mice by p53 and p21 null alleles. *Nature Genet.* **17**, 462-466.

Barlow, C., Brown, K. D., Deng, C.-X., Tagle, D. A. and Wynshaw-Boris, A. (1997b). Atm selectively regulates distinct p53-dependent cell cycle checkpoint and apoptotic pathways. *Nature Genet.* **17**, 453-456.

Bellvé, A. R. (1993) Purification, culture and fractionation of spermatogenic cells. *Meth. Enzymol.* **225**, 84-113.

Bishop, D., K,, Park, D., Xu, L. and Kleckner, N. (1992). DMC1: a meiosis-specific yeast homolog of E.coli *recA* required for recombination, synaptonemal complex formation, and cell cycle progression. *Cell* **69**, 439-456.

Bishop, D. K. (1994). RecA homologs Dmc1 and Rad51 interact to form multiple nuclear complexes prior to meiotic chromosome synapsis. *Cell* **79**, 1081-1092.

Boder, E. (1975). Ataxia-telangiectasia: some historic, clinical and pathologic observations. *Birth Defects* **11**, 255-270.

Brown, K. D., Ziv, Y., Sadanandan, S. N., Chessa, L., Collins, F. S., Shiloh, Y. and Tagle, D. A. (1997). The ataxia-telangiectasia gene product, a constitutively expressed nuclear protein that is not upregulated following genome damage. *Proc. Natl. Acad. Sci., USA* **94**, 1840-1845.

Carpenter, A. T. C. (1979). Recombination nodules and synaptonemal complex in recombination-defective females of Drosophila melanogaster. *Chromosoma* **75**, 259-292.

Chen, G. and Lee, E. Y. H.-P. (1996). The product of the ATM gene is a 370-kDa nuclear phosphoprotein. *J. Biol. Chem.* **271**, 33693-7.

Dobson, M. J., Pearlman, R. E., Karaiskakis, A., Spyropoulos, B. and Moens, P. B. (1994). Synaptonemal complex proteins: occurrence, epitope mapping and chromosome disjunction. *J. Cell Sci.* **107**, 2749-2760.

Dresser, M. E. and Moses, M. J. (1979). Silver staining of synaptonemal complexes in surface spreads for light and electron microscopy. *Exp. Cell Res.* **121**, 416-419.

Elson, A., Wang, Y., Daugherty, C. J., Morton, C. C., Zhou, F., Campos-Torres, J. and Leder, P. (1996). Pleiotropic defects in ataxia-telangiectasia protein-deficient mice. *Proc. Natl. Acad. Sci., USA* **93**, 13084-13089.

Hari, K. L., Santerre, A., Sekelsky, J. J., McKim, K., Boyd, J. B. and Hawley, R. S. (1995). The *mei-41* gene of D. melanogaster is a structural and functional homolog of the human ataxia telangiectasia gene. *Cell* **82**, 815-821.

Harlow, E. and Lane, D. (1988). *Antibodies: A Laboratory Manual*. Cold Spring Harbor: Cold Spring Harbor Laboratory Press.

Hogan, B., Beddington, R., Costantini, F. and Lacy, E. (1994). *Manipulating the MouseEmbryo: a Laboratory Manual*. Second Edition. Cold Spring Harbor: Cold Spring Harbor Laboratory Press.

Kastan, M. B., Zhan, Q., el-Deiry, W. S., Carrier, F., Jacks, T., Walsh, W. V., Plunkett, B. S., Vogelstein, B. and Fornace, A. J., Jr. (1992). A mammalian cell cycle checkpoint pathway utilizing p53 and GADD45 is defective in ataxia-telangiectasia. *Cell* **71**, 587-97.

Kato, R. and Ogawa, H. (1994). An essential gene, *ESR1*, is required for mitotic growth, DNA repair and meiotic recombination in *Saccharomyces cerevisiae*. *Nucl. Acids Res.* **22**, 3104-3112.

Keegan, K. S., Holtzman, D. A., Plug, A. W., Christenson, E. R., Brainerd, E. E., Flaggs, G., Bentley, N. J., Taylor, E. M., Meyn, M. S., Moss, S. B., Carr, A. M., Ashley, T. and Hoekstra, M. F. (1996). The Atr and Atm protein kinases associate with different sites along meiotically pairing chromosomes. *Genes Dev.* **10**, 2423-2437.

Kleckner, N. (1996). Meiosis: how could it work? *Proc. Natl. Acad. Sci., USA* **93**, 8167-8174.

Koehler, K. E., Hawley, R. S., Sherman, S. and Hassold, T. (1996). Recombination and non-disjunction in humans and flies. *Human Mol. Genet.* **5**, 1495-1504.

Lakin, N. D., Weber, P., Stankovic, T., Rottinghaus, S. T., Taylor, A. M. and Jackson, S. P. (1996). Analysis of the ATM protein in wild-type and ataxia telangiectasia cells. *Oncogene* **13**, 2707-16.

Lin, W.-C. and Desiderio, S. (1995). V(D)J recombination and the cell cycle. *Immunol. Today* **16**, 279-289.

Luna, L. G. (1992). *Histopathological Methods and Color Atlas of Special Stains and Tissue.* Gaithersburg: American Histolabs, Inc. Publications Division.

Lydall, D., Nikolsky, Y., Bishop, D. K. and Weinert, T. (1996). A meiotic recombination checkpoint controlled by mitotic checkpoint genes. *Nature* **383**, 840-843.

Meyn, M. S. (1995). Ataxia-telangiectasia and cellular responses to DNA damage. *Cancer Res* **55**, 5991-6001.

Moens, P. B., Chen, D. J., Shen, Z., Kolas, N., Tarsounas, M., Heng, H. H. Q. and Spyropoulos, B. (1997) Rad51 immunocytology in rat and mouse spermatocytes and oocytes. *Chromosoma* **105**, 207-215.

Orr-Weaver, T. L. (1995). Meiosis in *Drosophila*: seeing is believing. *Proc. Natl. Acad. Sci., USA* **92**, 10443-10449.

Pittman, D. L., Cobb, J., Schimenti, K. J., Wilson, L. A., Cooper, D. M., Brignull, E., Handel, M. A. and Schimenti, J. C. (1998) Meiotic prophase arrest with failure of chromosome synapsis in mice deficient for Dmc1, a germline-specific RecA homolog. *Mol. Cell* **1**, 697-705.

Plug, A. W., Peters, A., Xu., Y., Keegan, K. S., Hoekstra, M. F., Baltimore, D., deBoer, P. and Ashley, T. (1997) ATM and RPA in meiotic chromosome synapsis and recombination. *Nat. Genet.* **17**, 457-461.

Roeder, G. S. (1995). Sex and the single cell: meiosis in yeast. *Proc. Natl. Acad. Sci., USA* **92**, 10450-10456.

Roeder, G. S. (1997). Meiotic chromosomes: it takes two to tango. *Genes Dev.* **92**, 10450-10456.

Sedgewick, R. and Boder, E. (1991). Ataxia-telangiectasia. In *Handbook of Clinical Neurology*, (ed. P. Vinken, G. Bruyn and H. Klawans) pp. 347-423. New York: Elsevier Scientific Publishers.

Shiloh, Y. (1995). Ataxia-telangiectasia: closer to unraveling the mystery. *Eur. J. Hum. Genet.* **3**, 116-38.

Weinert, T. A., Kiser, G. L. and Hartwell, L. H. (1994). Mitotic checkpoint genes in budding yeast and the dependence of mitosis on DNA replication and repair. *Genes Dev.* **8**, 652-665.

Xu, Y., Ashley, T., Brainerd, E. E., Bronson, R. T., Meyn, M. S. and Baltimore, D. (1996). Targeted disruption of *ATM* leads to growth retardation, chromosomal fragmentation during meiosis, immune defects, and thymic lymphoma. *Genes Dev.* **10**, 2411-2422.

Xu, Y. and Baltimore, D. (1996). Dual roles of ATM in the cellular response to irradiation and in cell growth. *Genes Dev.* **10**, 2401-2410.

Yoshida, K., Kondoh, G., Matsuda, Y., Habu, T., Nishimune, Y. and Morita, T. (1998) The mouse RecA-like gene Dmc1 is required for homologous chromosome synapsis during meiosis. *Mol. Cell.* **1**, 707-718.